PROTEIN FOLDING IN LIVING CELLS AND UNDER PRESSURE

BY

ANNA JEAN WIRTH

DISSERTATION

Submitted in partial fulfillment of the requirements
for the degree of Doctor of Philosophy in Chemistry
in the Graduate College of the
University of Illinois at Urbana-Champaign, 2015

Urbana, Illinois

Doctoral Committee:

Professor Martin Gruebele, Chair
Professor Yann Chemla
Professor Prasanth Kumar Kannanganattu
Professor Deborah Leckband

ABSTRACT

Protein folding, the process through which proteins gain their functional structure, can be approached from the perspective of many disciplines. Starting with biology, we can probe how protein structure relates to function and consider how the fold of a protein interacts with the biological environment. From the chemical perspective, we can treat protein folding as a chemical reaction and study the thermodynamics and kinetics of the structural transition. With physics, we can understand the underlying forces that give rise to protein folding and use theory and simulation to describe the protein folding process on an atomic level. This thesis studies protein folding through the lens of all three of these fields with two interdisciplinary methodological themes: one at the interface of chemistry and physics and the other at the interface of biology and chemistry.

In section 1, we study in detail the kinetics of fast-folding reactions following pressure-jump perturbation and pair experiment with molecular dynamics simulations. The first chapter is a review of the effects of pressure on the structure of biomolecules as well as a brief literature review of pressure-probed protein folding kinetics. We see that the methodology to study pressure-jumps is generally limited by time-scale—very fast folding is hard to study by pressure—and chapter two presents an overview of a fast pressure-jump instrument that meets this challenge. Although this instrument was developed by the previous generation of graduate students, several significant improvements are summarized in the chapter with a detailed user manual for the instrumentation. Closing up the section, we use the fast pressure-jump instrumentation as well as temperature-jump instrumentation to study the microsecond pressure and temperature-jump refolding kinetics of the engineered WW domain FiP35, a model system for beta sheet folding. With a full complement of molecular dynamics experiments mimicking experimental conditions, we show that simulation and experiment are consistent with a four-state kinetic mechanism and highlight FiP35's position at the boundary where activated intermediates and downhill folding meet.

Section 2 focuses on the interface of biology and chemistry, where we study how the protein folding reaction is impacted by immersion in the crowded intracellular environment and explore whether perturbations to the intracellular folding landscape can be linked to protein function. A review of the forces at play in the intracellular environment and the role that ultra-weak "quinary" interactions play inside living cells is presented in chapter 4, which also includes a review of the most recent literature studying biomolecular dynamics in their native environments. In chapter 5 we study the time-dependence of protein folding inside living cells as probed by live-cell fluorescent microscopy. We find that both the rate of folding and the thermodynamic stability of yeast phosphoglycerate kinase (PGK-FRET) are cell cycle-dependent, a process strictly regulated in time, suggesting that the interplay between the intracellular environment and proteins may impact their function. In chapter 6, a new probe to study protein folding in the cell is explored, namely the GFP/ReAsH Forster resonance energy transfer (FRET) pair. We show that this FRET pair suffers from bleaching artifacts but that directly excited ReAsH is an appealing prospect for studying protein folding in living cells on fast and slow time-scales. Finally, chapter 7 builds on the work presented in chapter 5 and chapter 6 by seeking a protein candidate whose function and in cell folding dynamics are linked. Several constructs of p53, a transcription factor, are explored as potential candidates for answering the question of whether protein activity level indeed can correlate with stability in living cells.

ACKNOWLEDGEMENTS

I must thank first and foremost my advisor, Prof. Martin Gruebele, for his guidance over the past five years. I could not possibly list all the ways in which Martin has positively impacted my graduate career, but I especially want to express my gratitude for his receptiveness to new ideas and his scientific guidance. As I moved through my PhD it has become increasingly apparent how lucky I was to have an advisor like Martin—I cannot emphasize enough how grateful I am to have been a member of his research group.

Second, I owe much gratitude to those colleagues who trained me in the lab. Max Prigozhin taught me many of the techniques and instrumentation that have been the foundation of my PhD research. I'd especially like to thank Hannah Gelman for training me (and providing copious amounts of instrument support) on the live-cell instrumentation. Minghao Guo, as well, was particularly helpful with all sorts of instrumentation and analysis problems I experienced over the years. Irisbel Guzman Sanchez taught me how to do temperature-jump experiments as well as many biochemical techniques. I am also grateful to Max Platkov for his assistance with the PID.

I would also like to thank the members of the Gruebele group for their support and friendship: Krishnarjun Sarkar, Max Platkov, Eduardo Berrios, Kiran Girdhar, Ruopei Feng, Tatyana Perlova, Elaine Christman, Kapil Dave, Drishti Guin, Hannah Gelman, Maxim Prigozhin, Irisbel Guzman Sanchez, Minghao Guo, Jay Goodman, Shahar Sukenik, Timothy Chen, Yangfan Xu, Lea Nienhaus, Duc Nuygen, and Sumit Ashketar. I am honored to have worked with such excellent colleagues. In particular, I am very thankful to have been office-mates with Hannah Gelman and Irisbel Guzman Sanchez who have helped me so much over the past five years.

I also must thank several collaborators. On the pressure-jump project, I was fortunate to collaborate with Yanxin Liu and Prof. Klaus Schulten. I am grateful for Yanxin's excellent work and for the opportunity to access the Schulten group's computational prowess and resources. On my ReAsH work, I had the pleasure of working with my colleague Hannah Gelman.

I am greatly indebted to many staff in the School of Chemical Sciences. I would like to give special thanks to the entire administrative staff in the physical chemistry office who have been incredibly helpful throughout the years: Karen Watson, Beth Myler, Connie Knight, Theresa Struss, and Stacy Dudzinski. The SCS machine shop has been an invaluable resource that has solved an uncountable number of problems and crises. Tom and Mike "Hodge" Harland , especially, have made a significant impact in the success of the pressure-jump project. In the High Throughput Screening Facility, Cheng Zhang was a valuable resource for many years on our mammalian cell culture experiments.

My first research experiences were at the College of William and Mary under the direction of Prof. Lisa Landino, and I am grateful to have had the opportunity to get this early start in research. Prof. Landino's mentorship has been very valuable to me. I am also grateful for the guidance of Prof. Joel Hockensmith at the University of Virginia, whose mentorship during the SRIP program helped me form the foundation of my understanding of molecular biology. I'd also like to thank Prof. Carey Bagdassarian at the College of William and Mary, who was the first to teach me the joys of using computational tools and modeling to better understand nature.

Last, I must thank my family for all their support and love. Most of anything I have achieved springs from my luck of being born into such a wonderful family. My husband's family has also been supportive and helpful far beyond the call of duty. Finally, my husband, Daniel, has been a calming, supportive presence in my life who has made the stresses of graduate school bearable and life in Champaign-Urbana fun—its hard to imagine how I would have managed to finish my degree without him in my life.

TABLE OF CONTENTS

SECTION I: PROTEIN FOLDING UNDER PRESSURE

CHAPTER 1
PRESSURE PERTURBATION OF PROTEIN STRUCTURE

1.1 MECHANISM OF PROTEIN PRESSURE DENATURATION AND THE PRESSURE UNFOLDED STATE

1.1.1 Pressure-probed folding thermodynamics For over 100 years, it has been known that application of high pressures has an effect on protein structure. The discovery was first made by observing the coagulation of albumin, from an egg white, under pressure[1]. Since then, pressure has been used, although less popularly than temperature or denaturants, to probe structural transitions in proteins and other biomolecules, particularly oligomeric or aggregated proteins.

The effect of pressure on a protein's fold can be understood entirely through Le Chatelier's principle[2]: at high pressures, the energetically favored structure has the minimum volume. Generally speaking, the unfolded state of globular proteins is lower in volume than the folded state which gives rise to denaturation at high pressures.

The pressure dependence of the free energy of folding, ΔG, is given by:

$$\Delta G(P) = \Delta G_0 + \Delta V_0(P - P_m) - \frac{V\Delta\beta_T}{2}(P - P_m)^2$$

where ΔV_0 is the volume change upon unfolding, P_m is the pressure unfolding midpoint, and $\Delta\beta_T$ is the change in isothermal compressibility upon unfolding. Thus, while temperature denaturation accesses the enthalpy and heat capacity of a protein, a pressure denaturation thermodynamics experiment provides information on the volume change upon unfolding as well as the isothermal compressibility of the protein. Figure 1 shows a generic phase diagram for temperature and pressure denaturation of a protein and the trend in volume change exhibited for both denaturation methods.

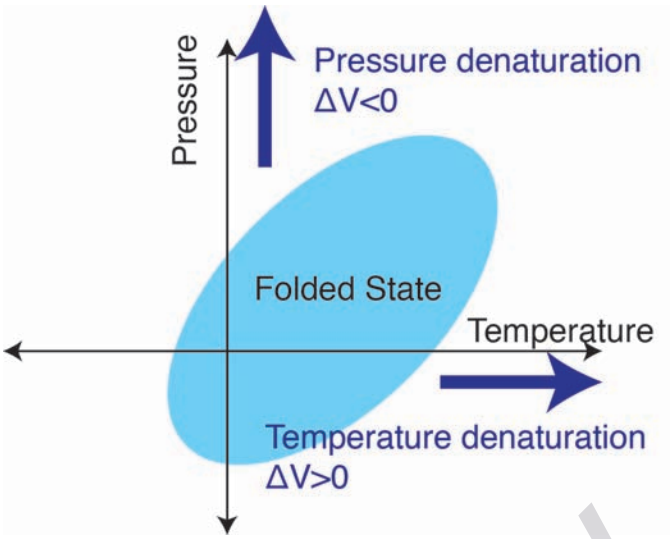

Figure 1 Temperature pressure phase diagram. Area in light blue shows the region of the phase diagram where the protein is folded. The border of the ellipse shows the T_m or P_m of the protein at any pressure or temperature, respectively.

1.1.2 The pressure unfolded state The contrast between the dependence of the free energy on temperature and the dependence of the free energy on pressure provides some insight into the often nuanced effect pressure can have on protein structure. While temperature denatures proteins by perturbing both volume and energy, pressure perturbs only volume, making it a somewhat more gentle denaturation method that can leave secondary structure behind in the unfolded state. Often, the radius of gyration of the pressure-unfolded ensemble is lower than what would be expected for a true random coil[3].

In an extreme example of residual secondary structure in the pressure-denatured state, a transcription factor in its pressure denatured state retained its globular structure—thus appearing fully folded by NMR measurements—but had its core completely penetrated by water—thus appearing completely unfolded by tryptophan fluorescence measurements[4]. Numerous examples of the pressure denatured state showing residual secondary structure, particularly alpha-helical structure, have been reported across the literature[3,5,6]. Indeed, it was shown that the volume change of unfolding for an isolated helical peptide is positive, suggesting that in some cases helices are stabilized at high pressures[7].

1.1.3 Origins of pressure-induced unfolding Until recently[8], the origin for the difference in volume between the folded and unfolded states of globular proteins (and, thus, the variation in the sensitivity of various protein folds to pressure denaturation) was poorly understood. Because protein

solutions are not ideal solutions, the change in molar volume upon unfolding is dependent on hydration effects as well as changes in volume due to the disruption of internal cavities that exist in the folded state. Solvent effects alone, including unfavorable solvation of non-polar groups at high pressures driving their packing in the core of the protein[9] and changes in the bulk structure of water at high pressures[10], cannot alone explain the difference in the molar volume between the folded and unfolded state[2]. A recent exhaustive high pressure NMR study of cavity forming mutants of staphylococcal nuclease showed that the susceptibility of proteins to high pressure derives mostly from the presence of internal cavities in the folded state[8]. Thus, the general consensus in the literature is that the higher the volume of internal cavities in a protein or the higher degree of packing defects in the fold, the more susceptible a protein is to pressure denaturation.

1.2 PRESSURE-PROBED PROTEIN FOLDING KINETICS

Pressure-probed kinetics can provide useful information about a protein's transition state through measurement of the activation volume, $\Delta V_f^{\ddagger}$, which is related to the measured pressure-probed folding rate, k_f, by:

$$k_f = k_m e^{-p\Delta V_f^{\ddagger}/RT}$$

where k_m is the folding prefactor and p is the pressure. The ratio of the folding activation volume and the overall volume change of folding, called the "V-value"[11], provides an estimate in the change in hydration between the unfolded state and the transition state. This measure is essentially the pressure analog to the Φ-value and provides a complimentary method to traditional T-jump and stopped-flow experiments to understand the nature of the transition-state.

Because the molar volume of the transition-state ensemble is higher than the unfolded state (or, in other words, the activation volume is very positive), proteins unfold very slowly at high pressures and upwards pressure-jumps greatly slow reaction kinetics [12]. The slowing of kinetics enables use of instrumentation that otherwise would have lacked the time resolution to observe the kinetics. For example, the folding of staphylococcal nuclease was measured with site-specific precision via upwards pressure-jumps monitored by multi-dimensional NMR[13]. Here, the rate of folding for each individual residue was resolved and used to show that pressure effects on the fold are observed in different regions of the protein structure depending on mutant and denaturant concentrations—remarkably specific mechanistic insight.

1.3 PRESSURE AND PROTEIN AGGREGATION

Aside from its obvious utility in studying protein folding from a mechanistic perspective, pressure has useful applications in understanding other biomolecules, including nucleic acids[14] and oligomeric proteins[15]. One area of active research is pressure's ability to disaggregate non-productive protein aggregates including amyloid fibrils and bacterial inclusion bodies.

1.3.1 Probing amyloid fibrils with pressure Amyloid fibrils are a type of protein aggregate that is common across many diseases, particularly neurodegenerative disorders, including Parkinson's Disease, Alzheimer's Disease, and Huntington's Disease. Amyloid fibrils are characterized by a beta-sheet topology that varies depending on the protein sequence that gives rise to the fibril. Until the past decade with the expansion of solid-state NMR techniques, amyloid fibrils were not understood structurally at the molecular level due to their poor crystallization and incompatibility with solution NMR[16].

Pressure, however, offers an interesting, and relatively straightforward, way to probe the general attributes of fibril structure. Because the structural stability of biomolecules to pressure denaturation depends on internal cavities, the resistance to pressure denaturation of fibrils can be used to probe the packing efficiency of the fibril structure[17]. Indeed, the stability of amyloid fibrils to application of high pressure is not uniform, reflecting the known diversity of fibril structure. In some cases, amyloid fibrils were found most sensitive to pressure denaturation early in the fibril formation process before eventually growing over more time resistant to even very high pressures, presumably due to internal reorganization that occurs over time and reduces packing deficiencies in the fibril structure[16,18]. In most other cases[14], however, amyloid fibrils were found to be very sensitive to pressure denaturation, the behavior of hen lysozyme fibrils being typical which shows accelerated dissociation under pressures as low as 50 MPa[19].

Even slight differences in fibril structure, as might be expected between amyloid fibrils formed from two mutants of the same protein, give rise to varying resistivity to applied pressure. A study on Alpha-Synuclein found that fibrils made from wild-type Alpha-Synuclein were more likely to resist denaturation than the mutant varieties that lead to inherited forms of Parkinson's Disease due to structural differences between the two types of fibrils[20]. This implied that the in cell protease machinery was more likely to be able to break up the mutant amyloid fibrils into smaller aggregates (which are thought to be more neurotoxic than the full-length fibrils), offering a possible

explanation for why those with inherited mutations have a more severe form of Parkinson's Disease than those with sporadic cases.

High pressure is also useful to study aggregation kinetics because it can often stabilize partially folded intermediates that otherwise would be too transient to observe. Aggregation or amyloid formation is often thought to originate from partially folded, off pathway intermediates, and high hydrostatic pressure has been proposed as a way to access these intermediates in order to better understand the early steps of the amyloid formation[21]. For example, in the case of transtheyretin, high pressure disaggregates fibrils into a partially folded intermediate that reaggregates upon return to atmospheric pressure more rapidly than the monomeric protein under aggregation-promoting conditions[20].

1.3.2 High pressure to purify proteins from inclusion bodies A common problem faced in the field of biotechnology are proteins that aggregate in bacterial expression systems. Rather than remain soluble in the bacterial cytoplasm, some proteins aggregate and amass into highly insoluble inclusion bodies from which purification of the target protein of interest is extremely difficult. The ability to purify difficult to express proteins at high yield is of great importance in the pharmaceutical industry, particularly as the development of biologics-based drugs becomes more prevalent.

Pressure's ability to disaggregate amyloid fibrils translates to the solubilization of inclusion bodies. Some of the first proteins to be folded from inclusion bodies by use of high pressure were human growth hormone, lysozyme, and beta-lactamase[22]. In many cases, very low concentrations of GuHCl and hydrostatic pressures of 20 MPa were sufficient to complete break up insoluble aggregates, and a return to GuHCl free buffer and atmospheric conditions resulted in complete refolding of the protein.

1.4 BRIDGING PRESSURE-JUMP EXPERIMENTS AND SIMULATIONS THROUGH LOW DEAD-TIME PRESSURE-JUMP INSTRUMENTATION

While simulated temperature-jumps[23] and long MD simulations at high temperatures where multiple folding and unfolding transitions can be observed[24,25] are relatively common place, simulations at high pressures[26,27] or of pressure-jumps[28,29] are rarer, despite the utility of comparing pressure-perturbation results with experiment to improve the performance of force fields. The reason for the paucity of pressure-jump simulated data is that, until recently, there were no experimental reports of pressure-probed kinetics with rates below a millisecond and, thus, no

experimental benchmark available for comparison to the simulated data. Although the pressure-probed kinetics of several protein systems have been thoroughly studied, namely the ankyrin repeat protein[30,31], staphylococcal nuclease[11,13,32,33], and lambda repressor[28,34,35], only the lambda repressor has a kinetic phase less than a millisecond.

The biggest challenge to measure the pressure-induced kinetics of fast folders is instrumentation. Figure 2 summarizes the major types of pressure-jump instrumentation and highlights the differences in the size of the pressure-jumps the instrumentation is capable of administering and the fastest kinetics that can be resolved. The most common strategy to administer pressure changes is through the use of valve-based instrumentation. While this enables large jumps in pressure, the dead-time of most electrically-controlled valves or "fast-valves" in figure 2 is on the order of 5 milliseconds[36]. For a downward pressure-jump, this limits the studied proteins to those that fold on the order of 10's of milliseconds.

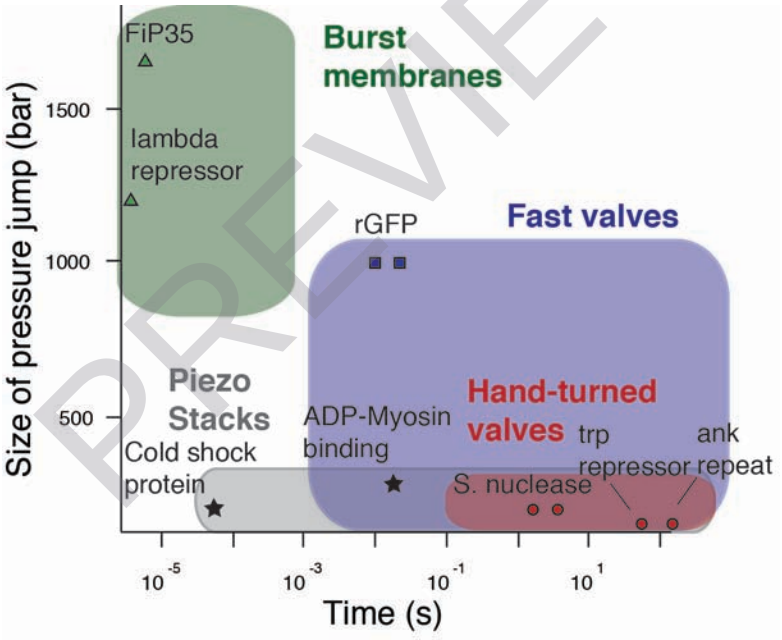

Figure 2 Summary of the three major types of pressure-jump instrumentation. For each method, the ranges of the pressure-jump size administered and kinetic rate resolution possible are indicated by the borders of the colored regions. Examples of kinetic rates observed for each method type are shown. The references for the various proteins are: Staphylococcal nuclease[11,32], ankyrin repeat protein[30], trp repressor[6], lambda repressor[28,35], Myosin-ADP binding[37], and cold shock protein[38]. Fip35 is the subject of chapter 3 of this thesis.

One useful strategy to circumvent the time-scale limitations of valve-based instrumentation is to employ upwards pressure-jumps. At high pressures, protein folding reactions proceed at a much slower rate, so instrumentation dead-time becomes less critical for resolving reaction kinetics.

In this case, hand-controlled valves can be used to administer jumps of up to a few hundred bar and monitor reaction kinetics with rates as fast as a few seconds (red highlighted area in figure 2). Upward pressure-jumps are particularly useful because reactions can proceed so slowly that kinetics can be monitored by multi-dimensional NMR, which allows residue by residue monitoring of protein folding transitions[13]. However, while slowing down the kinetics makes them easier to measure, this strategy is incompatible with directly comparing experiment to molecular dynamics simulations.

Chapter 2 of this thesis describes in detail a burst-membrane based approach to measure fast folding kinetics following pressure-drop. As is highlighted in figure 2, burst-membrane based instrumentation can access protein folding rates on the order of microseconds. In Chapter 3, this instrumentation is used to study the fast folding of FiP35 following pressure-jump and the resulting kinetics are directly compared to molecular dynamics simulations of pressure-jumps.

CHAPTER 2
PRESSURE-JUMP INSTRUMENTATION TO STUDY PRESSURE-PROBED MICROSECOND FOLDING KINETICS

2.1 INTRODUCTION

Previously, the Gruebele group developed a burst-membrane based pressure-jump instrument that enables very large pressure drops—exceeding 2000 times atmospheric pressure—with an instrument dead-time of only 1 μs. With such resolution and jump size, the instrument has been used to measure the pressure-probed folding kinetics of fast folders including lambda repressor[28,34,35] and the WW-domain mutant FiP35 (Chapter 3). In the case of Lambda repressor[28,35] and FiP35 (Chapter 3), the resolved pressure-jump kinetics were fast enough to be compared directly to molecular dynamics simulations, which is only possible due to the microsecond dead-time of the pressure-jump instrumentation. From the original prototype reported in Nature Methods[34], a number of improvements to the instrumentation were made that enabled greater ease of use and, accordingly, higher throughput. Building upon these improvements, the work presented in chapter 3 represents an approximately 5-fold increase in the number of measurements obtained in a typical experimental run. The first section of this chapter summarizes the major instrument improvements and provides rationale for why they were needed. The remaining sections provide a detailed overview of assembly and operation of the pressure-jump instrumentation. Appendix D includes a troubleshooting guide for users which covers all major (and minor) problems encountered over the past 5 years.

2.2 IMPROVEMENTS MADE TO THE PRESSURE-JUMP INSTRUMENTATION

2.2.1 Laser stability Originally, the pressure-jump apparatus was mounted onto the optical table that is shared by the Ti:Saph laser, which provides (see section 2.4) the excitation source for fluorescence detection of protein folding. In order for the laser signal to be frequency tripled to tryptophan's 280 nm excitation maximum and to effectively trigger signal collection on the scope, the laser is mode-locked with a pulse train at 80 MHz. The stability and reliability of this mode-lock can be perturbed by shocks to the optical table.

The pressure drop instrumentation for jumps greater than 1000 bar delivers a significant shock to the table that often perturbs the mode-lock enough to interfere with signal collection. Several strategies were employed to avoid this problem including mounting the pressure-jump

apparatus onto a piece of shock absorbing honeycomb steel and attaching this breadboard to the optical table with shock absorbing rubber feet. While this was effective, the limited lifetime of the rubber feet (<1 year) made this approach non-sustainable.

The solution that has proved most effective in the long term is mounting the pressure-jump instrument to its own pedestal separate from the optical table. This pedestal is firmly mounted to the concrete floor via screws and the only connections between the shock-producing pressure-jump instrument and the optical table are flexible wires and a pmt light-guide. By mechanically isolating the pressure-jump assembly from the sensitive optical equipment, large jumps can now be accessed (as high as 3000 times atmospheric pressure), without laser disruption.

2.2.2 Signal corruption One persistent problem with the pressure-jump instrument has been random electrical noise evident in the fluorescent signal. This typically manifests itself as large baseline rolls in the signal that appear right around the jump. Many different hypothesis for the origin of this signal corruption were tested and ruled out including: 1) Contamination of the fluorescence signal by stray light from sparks (which occur when the membrane breaks), 2) Mechanical oscillation of the pressure-jump assembly causing the laser path length through the sample to change, 3) Mechanical disruption of the laser signal, and 4) Electrical artifacts from the capacitor bank discharge travelling to electrical equipment through the metal optical table. Ultimately, it was determined that the problem arises from electrical interference originating from the extremely large capacitor bank discharge partially through the air and partially through the electrical connections. The PMT appears to be exquisitely sensitive to these random electrical signals. The best strategies to combat this kind of electrical interference are to a) use the Faraday cage around the capacitor bank and P-jump assembly, b) ensure that the fluorescence signal is extremely robust (>100 mV on the scope) so that interference doesn't overwhelm the signal, and c) use signal processing to remove some electrical noise that breaks through the signal. These strategies are discussed in detail in Appendix D.

2.2.3 Equipment changes A number of changes were made to the equipment used throughout the instrument including the materials of the pressure fitting, the method the sample cavity is machined into the sapphire cube and the design of the non-conductive cylinder. These improvements are outlined in section 2.3.

2.3 PRESSURE-JUMP INSTRUMENT COMPONENTS

2.3.1 Pressure fitting

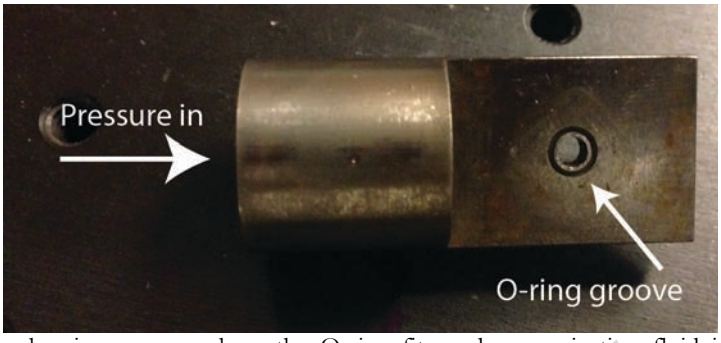

Figure 3 Pressure fitting showing groove where the O-ring fits and pressurization fluid inlet. The liquid emerges through the hole surrounded by the O-ring groove, which is placed above the sample.

What it does: Guides pressurization fluid to sample

Replacement guidelines: The area around the O-rings becomes corroded due to the electrical discharge (which can essentially weld the steel burst membrane to the pressure fitting) and this can lead to O-ring damage. When O-rings start breaking frequently, it's time to replace the pressure fitting. These shouldn't need to be replaced more than once a year with typical instrument usage. The SCS machine shop makes this part and has a diagram on file. It should be made of steel and then hardened. Titanium is also acceptable.

2.3.2 Sapphire cube

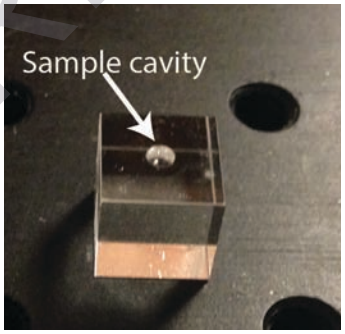

Figure 4 Sapphire cube with machined sample cavity. The sample cavity typically holds 5-10 μL of sample. The diameter of the sample cavity is slightly smaller than the diameter of the o-rings, enabling the bottom o-ring to form a seal around the edge of the sample cavity.

What it does: Holds the sample. Sapphire is used because it is strong and optically transparent.

Replacement guidelines: Sapphire cubes can be used until they break. Even cracked cubes can sometimes continue to be used for a long time provided the crack does not cross through the sample cavity. We order the sapphire cubes from Esco products and they have the measurements and specification on file. The sample hole is machined into the cube by the machine shop. The hole should be smaller in diameter than the O-ring and on the strong face of the sapphire. Finding the strong face:

1) Put a polarizer on a flashlight and turn on the flashlight
2) Set a cube on the polarizer
3) Hold the other polarizer on top and rotate it.
4) Watch the top face of the cube. If you have found a strong face, there will be a spectrum of many colors visible as you rotate the polarizer. The opposite face will have the same spectrum.
5) A weak face shows no color spectrum.

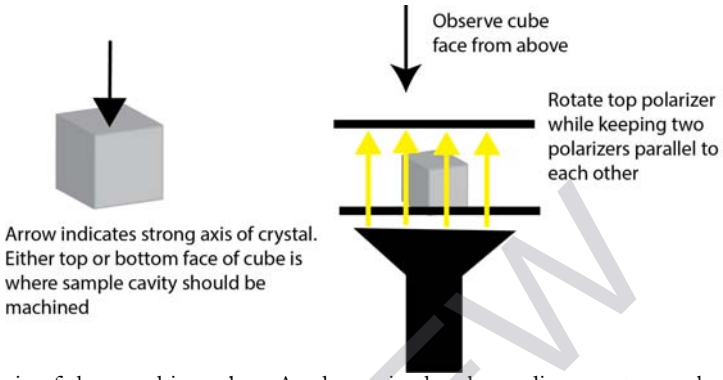

Figure 5 Finding the strong axis of the sapphire cubes. As shown in the above diagram, two polarizers and a flashlight can be used to identify the directionality of the crystal so that the strongest axis is used for machining of the sample cavity.

2.3.3 Burst membrane

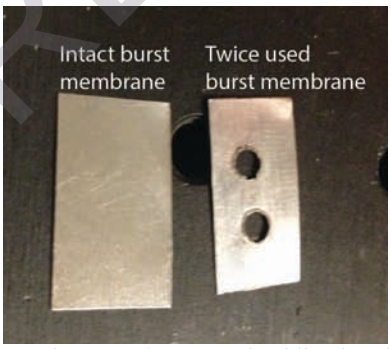

Figure 6 Burst membrane. Left membrane has not been used while the right membrane has been used twice, as evidenced by the two burst holes. The clean edges of the burst holes indicate that the jump was likely with a low dead-time.

What it does: Breaks when capacitor charge is delivered and allows the system pressure to drop very rapidly.

Replacement guidelines: These can be used twice (put the membrane into the assembly another way so that un-burst steel is over the sample cavity). We buy stainless steel shim stock to cut into burst membranes from McMaster Carr. One order from McMaster Carr will supply enough membranes

for several hundred or more jumps. In a pinch, the SCS machine shop usually has some shim stock. 5-7 thousands of an inch thick stock can be cut with scissors into membrane sized pieces. These thicknesses access the range of jumps from 1000 to 2000 bar. Thicker shim stock can be cut in the machine shop with shears. The membrane should be about the width of a cube and 2/3 the length of the tongue of the pressure fitting.

2.3.4 Foil

Figure 7 Foil used to protect the sample from contamination by pressurization fluid. Visible here is the folded piece of aluminum coated Mylar that wraps around a piece of foil.

What it does: Protects the sample from the pressurization fluid and blocks sparks that form when the membrane bursts from contaminating the fluorescence signal.

Replacement: These need to be replaced every other jump or so. To make, wrap a piece of aluminum coated Mylar around a piece of foil. It helps to wet the Mylar so it sticks to the foil. To restock foil, Sigma sells many kinds of foil that can be used for the inner piece. The aluminum wrapped Mylar is an emergency blanket (the kind that marathon runners use after races).

2.3.5 Electrode

Figure 8 Copper electrode. Tips on either end are sharpened in order to cleanly break the burst-membrane. The double ended design allows a single electrode to be used twice before needing to be re-machined.

What it does: Copper electrode with sharpened tips on both sides. Delivers capacitor discharge to burst membrane.

Replacement guidelines: These can only be used once per side before they need to be re-machined. The end that comes into contact with the burst membrane must be sharp, or the break will not be clean.

The machine shop makes this part and can re-furbish old electrodes until they are too short to reach from the top of the pressure assembly to the burst membrane. A part diagram is on file at the machine shop and the material used is copper.

2.3.6 Non-conductive cylinder

Figure 9 Non conductive cylinder. This cylinder is seen from the top, where the electrode enters the cylinder before making contact with the burst membrane. The groove is meant to enable liquid that escapes during the pressure drop to travel away from the electrode.

What it does: Specially treated, heat and pressure resistant piece of ceramic that guides the electrode to the burst membrane. As the burst membrane is weakened by the pressure, it pushes up into the bottom of the cylinder so the cylinder also determines the size of the hole that is burst in the burst membrane.

Replacement guidelines: These can be used for approximately 50 jumps. When the edges of the hole on the bottom are no longer sharp, the jump resolution will suffer and its time for the cylinder to be replaced. These are ordered from AstroMet and all the information should be on file there. It is essential that the bottom of the through hole of the cylinder (where it contacts the burst membrane) is sharp and does not have a chamfer. Otherwise, sapphire cubes will break and jump resolution will be poor.

2.3.7 O-ring

What it does: Provides a seal between the pressure fitting and the foil and the pressure fitting and the burst membrane.

Replacement guidelines: These last a variable amount of time. Only replace if they are obviously broken or pressure is not holding well in the assembly. They are .158 x .02090 o-rings made of fluorocarbon from Apple Rubber Products (part number R00158-020-90VTB).

2.3.8 High pressure tubing, pressure fitting connector, and nipple

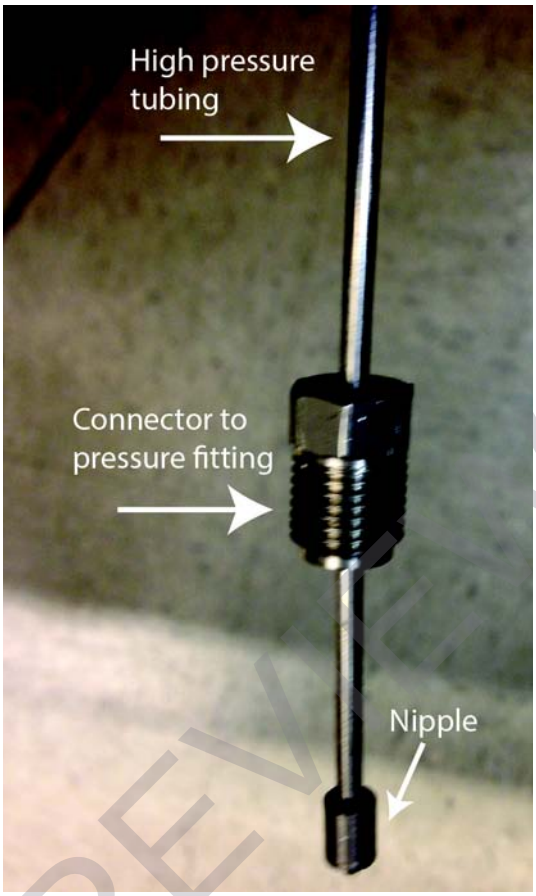

Figure 10 High pressure tubing diagram showing the end of the tubing. The nipple is attached via threading on the end of the high pressure tubing. The connector to the pressure fitting slides over the nipple, enabling a tight seal to form between the pressure-jump instrument and the high pressure tubing.

What it does: Connects pressure generator to the pressure-jump assembly and delivers pressurization fluid.

Replacement guidelines: Replace the tubing when it starts functioning poorly. Common problems are leaks, usually where the tubing has been bent, and clogs. The tubing can be purchased from High Pressure Equipment Company (HiP). Make sure to buy tubing that is rated for at least 3000 bar. The channel is machined here to add threads to either end so that the nipple end piece can be attached. Nipples and pressure fitting connectors rarely need replacing.

2.4 SAFETY

2.4.1 Capacitor bank

The capacitor bank is an electrocution risk. Always make sure to discharge and turn off the capacitor before touching anything connected to it. Even if it discharged during the experiment, discharge

again (by switching the discharge button) and turn it off before disconnecting the assembly. It is a good practice to attach or detach the electrical contacts to the P-jump assembly with one hand. Never try to increase the pressure or adjust any aspect of the P-jump assembly when the capacitor bank is charged and connected to the assembly!

2.4.2 Laser

The laser beam moves upwards through the pressure assembly and towards your face, so take care when aligning the beam. Always block the beam path when you are working on the pressure assembly in case the shutter opens. Always keep the shutter closed (except during alignment), but bear in mind that static electricity can (and does) occasionally cause the shutter to spontaneously open and close.

2.4.3 Pressure

A pressure release not initiated by a capacitor discharge as might occur during pressurization is not violent but does release a lot of pressurization fluid like a little geyser. When using ethanol as a pressurization fluid and working close to the pressure assembly, it's a good idea to wear glasses or goggles. The pressure release with the capacitor discharge generates significant sparks, so no one should be near the pressure assembly during an experiment. Keep flammable materials (for example, ethanol soaked tissue) away from the pressure assembly.

2.5 OPERATION INSTRUCTIONS

2.5.1 System overview

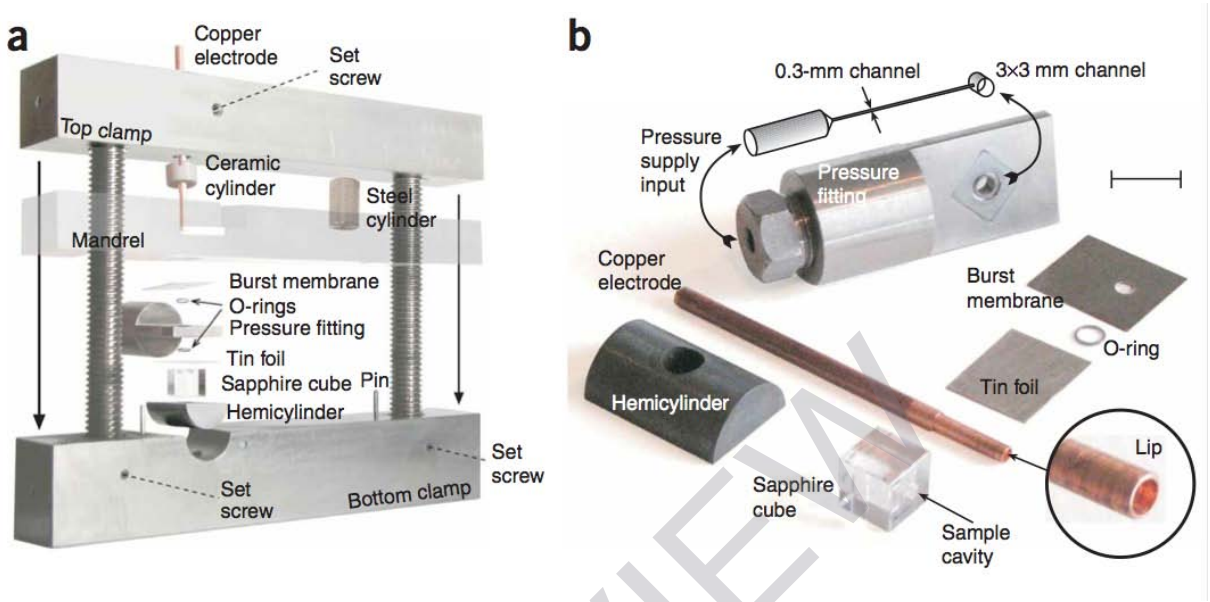

Figure 11 Pressure-jump assembly overview showing parts and their assembly. Figure from ref.[34]

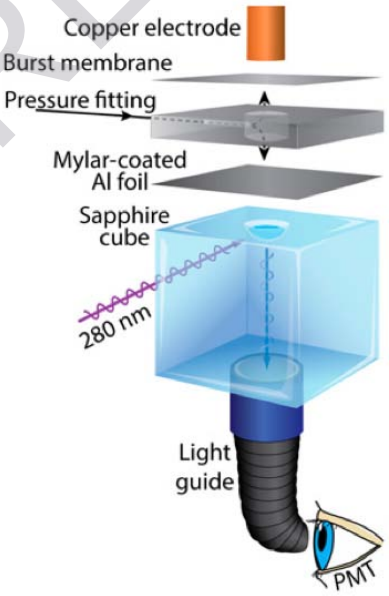

Figure 12 Schematic showing excitation and emission collection geometry relative to P-jump components. Figure from ref.[35]

2.5.2 Alignment of the laser in the pressure assembly

1) Get laser aligned, mode locked, and stable. Power from the tripler should be at least 10 mW.

2) Send the laser through the optics between the shutter and the pressure assembly. Make sure that the beam is centered in every mirror and the lens.

3) Place a card in the empty pressure-jump assembly. Roughly align the laser to be centered where the top of the cube will be. Adjust the placement of the lens in the beam path, if necessary, so that the beam is focused in the center of the sample cavity.

4) Put a concentrated tryptophan solution into the sample cavity of the cube and put the cube into the mantle and into the assembly. Adjust the alignment using the final mirror so that the beam moving through the sample. The beam should be clearly visible in the tryptophan solution.

5) Check the PMT alignment by ensuring that there is plenty of signal with the tryptophan only solution. If the signal is low, check the placement of the pmt light guides both in the assembly and at the PMT itself.

2.5.3 Using the pressure generator

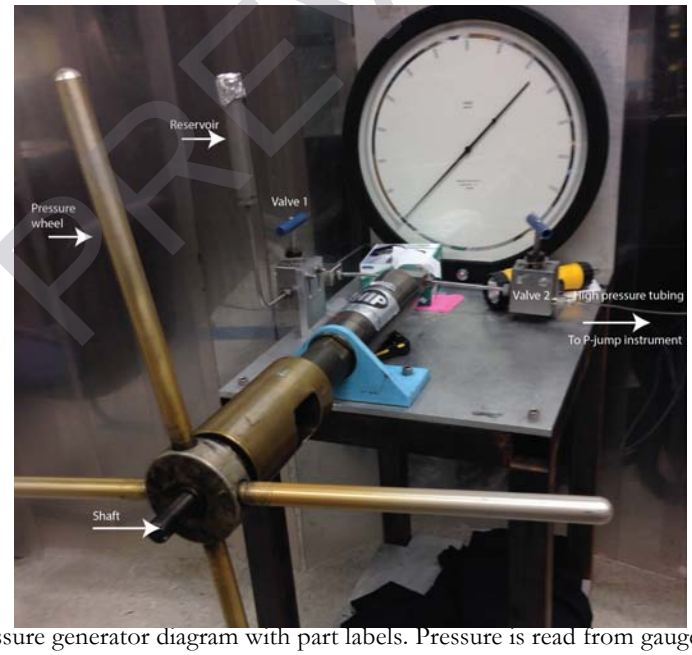

Figure 13 Hydrostatic pressure generator diagram with part labels. Pressure is read from gauge in center.

1) Make sure reservoir is filled with water or ethanol (either works fine, but if you switch between the two the system must be primed completely with the new pressurization fluid).

2) If the shaft is not visible, the system needs to be primed. If the shaft is fully exposed, the system is ready to use (in the diagram above, the system is ready to use).

3) To prime the system: Turn the reservoir valve (valve one) to the fully open position (turn counter clockwise until it stops). Turn valve two to the fully closed position (turn clockwise until it stops). Turn the pressure wheel counter clockwise until it stops. This fills the pressure generator tubing with pressurization fluid from the reservoir. Close valve one and open valve two. The system is primed and ready to go.

4) To pressurize: Make sure valve one is closed and valve two is open. Turn the pressure wheel clockwise and watch the outlet to make sure pressurization fluid comes out. Connect the pressure assembly and start pressurizing by continuing to turn the pressure wheel clockwise. Watch the gauge to monitor pressure.

5) To pressurize again, repeat steps 3 and 4.

6) NOTE: watch the shaft carefully. If it is not-visible, it's time to prime the system. If you turn too far, the wheel can come off.

2.5.4 Putting together the pressure assembly and pressurizing

1) Insert the cube into the mantle ("mantle" is called "mandrel" in the Nature Methods paper) and the mantle into the assembly.

Mantle in lowered position with cube inserted:

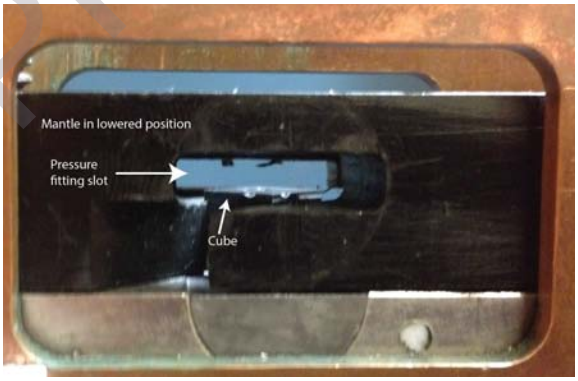

Figure 14 Assembly step 1. Cube is inserted with the slot for the pressure fitting clearly visible.

2) Carefully add just enough sample to fill the sample cavity with a pipette (access through the top).

3) Raise the mantle about .5 cm, leaving the cube in place.

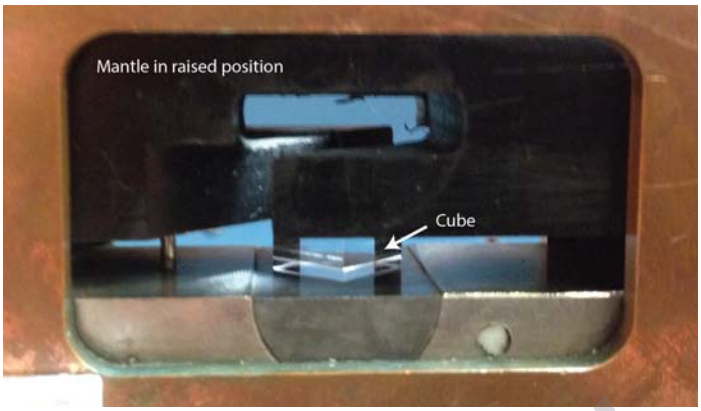

Figure 15 Assembly step 3. Mantel in raised position to facilitate easy insertion of the pressure fitting.

4) Place the foil carefully into the pressure fitting slot with tweezers. The foil should be slightly narrower than the pressure fitting and about 2 or 3 times as long as the width of the cube.

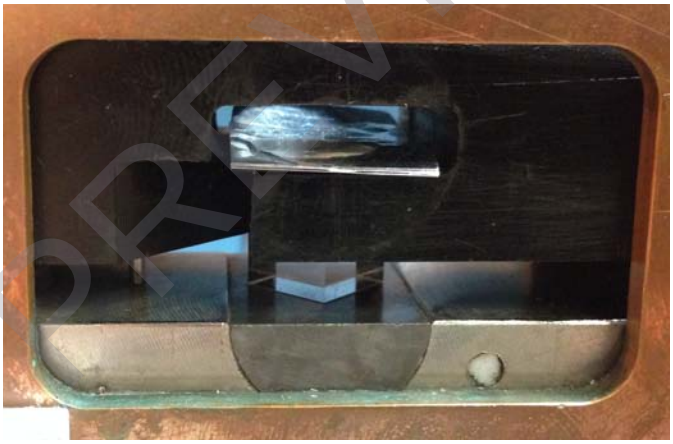

Figure 16 Assembly step 4. Mantel in raised position with foil inserted.